Gap junction protein connexin-43 interacts directly with microtubules

Ben N.G. Giepmans*, Ingrid Verlaan*, Trudi Hengeveld*, Hans Janssen†, Jero Calafat†, Matthias M. Falk‡ and Wouter H. Moolenaar*

Gap junctions are specialized cell-cell junctions that mediate intercellular communication. They are composed of connexin proteins, which form transmembrane channels for small molecules [1, 2]. The C-terminal tail of connexin-43 (Cx43), the most widely expressed connexin member, has been implicated in the regulation of Cx43 channel gating by growth factors [3–5]. The Cx43 tail contains various protein interaction sites, but little is known about binding partners. To identify Cx43-interacting proteins, we performed pull-down experiments using the C-terminal tail of Cx43 fused to glutathione-*S*-transferase. We find that the Cx43 tail binds directly to tubulin and, like full-length Cx43, sediments with microtubules. Tubulin binding to Cx43 is specific in that it is not observed with three other connexins. We established that a 35-amino acid juxtamembrane region in the Cx43 tail, which contains a presumptive tubulin binding motif, is necessary and sufficient for microtubule binding. Immunofluorescence and immunoelectron microscopy studies reveal that microtubules extend to Cx43-based gap junctions in contacted cells. However, intact microtubules are dispensable for the regulation of Cx43 gap-junctional communication. Our findings suggest that, in addition to its well-established role as a channel-forming protein, Cx43 can anchor microtubule distal ends to gap junctions and thereby might influence the properties of microtubules in contacted cells.

Addresses: *Division of Cellular Biochemistry and †Division of Cell Biology, The Netherlands Cancer Institute and Center for Biomedical Genetics, Plesmanlaan 121, 1066 CX Amsterdam, The Netherlands. ‡Department of Cell Biology, The Scripps Research Institute, La Jolla, California 92037, USA.

Correspondence: Wouter H. Moolenaar
E-mail: wmoolen@nki.nl

Received: **29 June 2001**
Revised: **25 July 2001**
Accepted: **27 July 2001**

Published: **4 September 2001**

Current Biology 2001, 11:1364–1368

0960-9822/01/$ – see front matter

Results and discussion

Increasing evidence indicates that gap-junctional Cx43 is part of a multiprotein complex. For example, the c-Src and v-Src tyrosine kinases can bind directly to and phosphorylate the Cx43 C-terminal tail (CT) via SH2 and SH3 domain interactions [6, 7]. Furthermore, the very C-terminal residues of Cx43 interact with the second PDZ domain of the Zona-Occludens-1 (ZO-1) protein, which may recruit regulatory proteins into gap junctions [8, 9]. Thus, the Cx43 complex might fulfill functions that are not necessarily related to the control of gap-junctional communication (GJC), a possibility that has received little attention to date.

To identify new Cx43 binding proteins, lysates of ^{35}S-Met/Cys-labeled Rat-1 cells were subjected to pull-down assays using the C-terminal tail of Cx43 fused to GST as an affinity matrix (GST-Cx43CT; Figure 1). Results of a typical experiment are shown in Figure 2. The most prominently labeled protein that interacts with Cx43CT, but not with GST alone, has an apparent MW of about 55 kDa (Figure 2a). When analyzed by two-dimensional SDS-PAGE/iso-electric focusing, at least 12 distinct Cx43CT-interacting protein spots were detected, among which was an intensely labeled 55-kDa spot (pI value 4.8; Figure 2b). In large-scale pull-down experiments, we detected a 55-kDa protein doublet on Coomassie-stained gels that corresponds to the ^{35}S-labeled 55-kDa protein (Figure 2c). The lower 55-kDa band was subjected to tryptic digestion. Sequence analysis of three distinct peptides revealed that the protein is identical to rat β-tubulin (Figure 2d). A trace amount of peptide was found to represent α-tubulin. Since α-tubulin migrates slightly slower than β-tubulin, the small amount of α-tubulin detected is probably derived from the upper band of the 55-kDa doublet. Immunoblot analysis of GST-Cx43CT pull-downs from ^{35}S-Met/Cys-labeled cell lysates confirmed the association of β-tubulin with Cx43 (Figure 2e). The association between Cx43CT and tubulin was also observed in lysates from rat liver epithelial T51B cells (see below), human fibroblasts, MDCK, COS7, A431, and HEK293 cells. These results demonstrate that tubulin interacts with the C-terminal tail of Cx43 in vitro.

To examine whether the interaction between Cx43 and tubulin is direct, we performed microtubule sedimentation experiments. As shown in Figure 3a, GST-Cx43CT cosediments with microtubules prepared in vitro (taxol-stabilized), whereas an irrelevant GST fusion protein

Figure 1

A schematic representation of Cx43 and constructs used in this study. The Cx43 sequence with the four transmembrane domains (TM) and the various Cx43 constructs are represented with the residue numbers indicated. C-terminally Myc-tagged constructs and N-terminally GST-tagged constructs are shown. JM, juxtamembrane domain; CT, C-terminal tail; GST, Gluthathion-*S*-transferase; aa, amino acid.

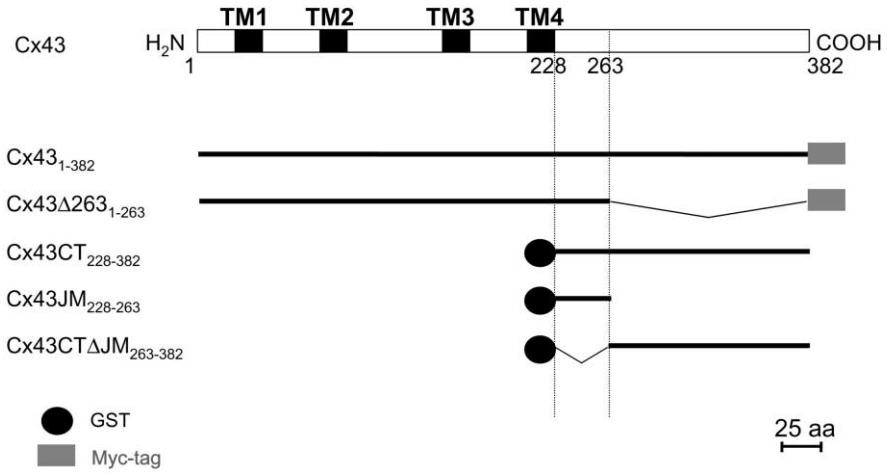

Figure 2

Proteins pulled down by GST-Cx43CT and identification of tubulin as the major Cx43CT binding protein. Lysates from ^{35}S-Met/Cys-labeled Rat-1 cells were subjected to pull-down assays using GST-Cx43CT or GST coupled to gluthathione-Sepharose beads. **(a)** Precipitated proteins were separated by SDS-PAGE and visualized by autoradiography. **(b)** Two-dimensional SDS-PAGE/IEF analysis of proteins precipitated with GST-Cx43CT. GST binding proteins (left panel) are encircled (white) in the GST-Cx43CT autoradiogram (right panel). Twelve Cx43CT binding protein spots are numbered and encircled in black. Spots 1 and/or 2 are likely to represent ZO-1 (predicted MW 195 kDa, pI 4.6). Spot 7 is the 55-kDa protein. **(c)** Large-scale pull-down from Rat-1 cell lysates with GST alone (30 kDa; lane 2) or GST-Cx43CT (43 kDa; lane 4) coupled to gluthathione-Sepharose beads. The 55-kDa protein (arrowhead) was isolated and further processed. Lanes 1 and 3 show GST and GST-Cx43CT fusion proteins prior to pull-downs. **(d)** The lower band of the 55-kDa doublet indicated in Figure 2b was subjected to in-gel trypsinization, and the resulting peptides were separated by reverse-phase HPLC (upper panel). Peptides in the indicated peak (arrowhead) were subjected to Edman degradation (middle panel). The recovered sequences are identical to those in rat β-tubulin. A trace amount of peptide in the indicated HPLC fraction was found to represent α-tubulin. **(e)** Identification of β-tubulin in GST-Cx43CT pull downs from metabolically labeled Rat-1 cells. Samples were separated by SDS-PAGE and transferred to nitrocellulose. Proteins were visualized by PonceauS staining (left panel) and autoradiography (middle panel). Subsequently, the blot was probed with anti-β-tubulin antibody (right panel).

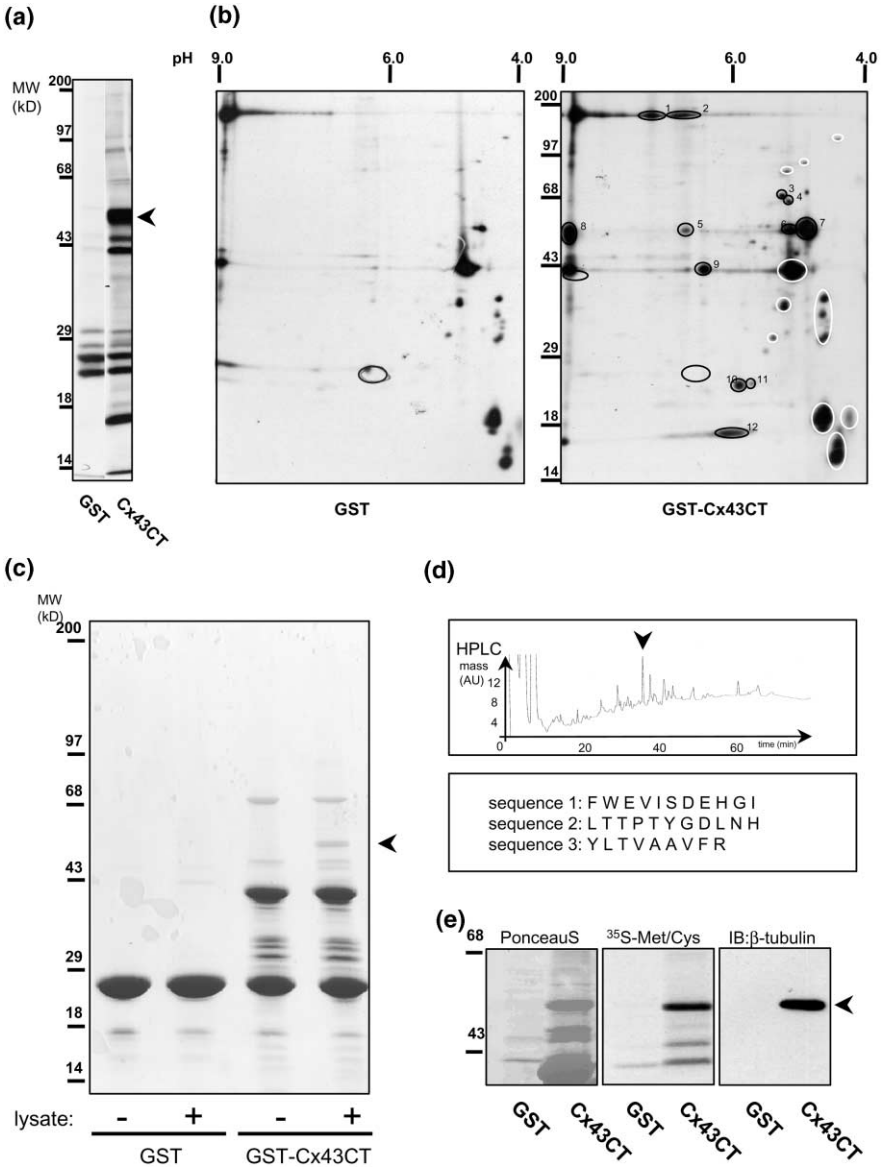

Figure 3

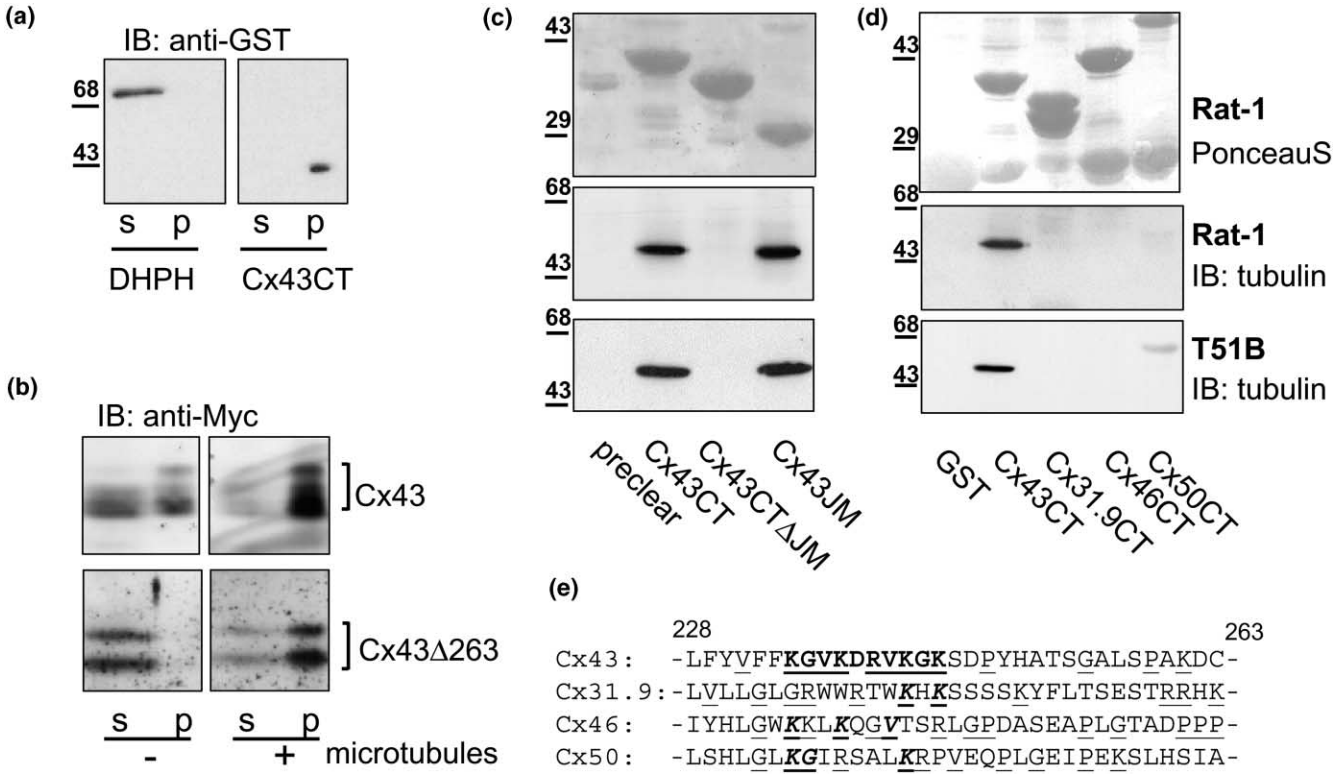

Cx43 interacts with microtubules via its unique C-terminal JM region. **(a)** GST-Cx43CT (43 kDa) cosediments with microtubules. In vitro-prepared microtubules were incubated with a control GST fusion protein (DHPH; 72 kDa; [17]) or GST-Cx43CT. Microtubules were pelleted by high-speed centrifugation. Supernatant (S) and pellet (P) fractions were subjected to SDS-PAGE and immunoblotted with anti-GST antibody (left). **(b)** Both full-length Cx43 and Cx43Δ263 cosediment with microtubules. Myc-tagged Cx43 and Cx43Δ263 were expressed in COS7 cells. Lysates were clarified by high-speed centrifugation. When microtubules are added (right panels), Cx43 (upper panel) and truncated Cx43 (lower panel) cosediment with microtubules into the pellet fraction (P). In the absence of microtubules, Cx43 and the truncation mutant (30 kDa) are found to a much lesser extent in the supernatant (S). **(c)** Mapping of the tubulin binding site to the unique JM region of Cx43. Pull-down assays in Rat-1 (middle panel) and T51B (lower panel) cell lysates, showing that Cx43CT binds to endogenous tubulin (lane 2). No tubulin binding is detected when the JM region (aa 228–263) in Cx43CT is deleted (Cx43CTΔJM) (lane 3). Lane 4 shows that the isolated JM peptide fused to GST (GST-Cx43JM) brings down tubulin to similar amounts as Cx43CT. Upper panel shows PonceauS staining of the fusion proteins used. **(d)** Connexin-specificity of tubulin binding. Pull downs were performed as in (c), using GST fusion proteins of the C-terminal tails of Cx43, Cx31.9, Cx46, and Cx50, as indicated. PonceauS staining of the fusion proteins is shown in the upper panel. It can be seen that tubulin is only pulled down by Cx43CT, but not by the corresponding tails of other connexin family members. **(e)** Putative tubulin binding sequence (bold) within the JM region of Cx43. This sequence is not conserved in other connexin family members (shown are Cx31.9, Cx46, and Cx50). Amino acids that are often enriched in tubulin binding sites are underlined.

(DHPH) does not. This indicates that the interaction between the Cx43 tail and tubulin is direct. We next examined whether the full-length Cx43 protein also binds to microtubules and, furthermore, which region in Cx43CT mediates tubulin binding. To this end, we generated C-terminally Myc-tagged Cx43 and a truncated version of Cx43 that lacks C-terminal residues 263–382 (Cx43Δ263; Figure 1). After expression of the constructs in COS7 cells, lysates were made and clarified to deplete insolubilized microtubules and connexins. Subsequently, microtubules prepared in vitro were incubated with the supernatant and then pelleted. As shown in Figure 3b (upper panels), Cx43 is strongly enriched in the pellet when microtubules are present. Strikingly, the C-terminally truncated mutant Cx43Δ263 also cosediments with microtubules (Figure 3b, lower panels). The sequences of Cx43Δ263 and GST-Cx43CT overlap only in the C-terminal juxtamembrane region (JM, 35 residues). We therefore generated GST-Cx43JM and GST-Cx43CTΔJM, which lacks the JM region (Figure 1). While the GST-Cx43CTΔJM protein fails to interact with microtubules, the isolated JM region (GST-Cx43JM) binds tubulin to the same extent as Cx43CT (Figure 3c). Thus, the tubulin binding domain of Cx43 is located within the 35-amino acid juxtamembrane region of the C-terminal tail.

In general, microtubule binding domains are basic and enriched in lysine, valine, proline, and glycine residues

Figure 4

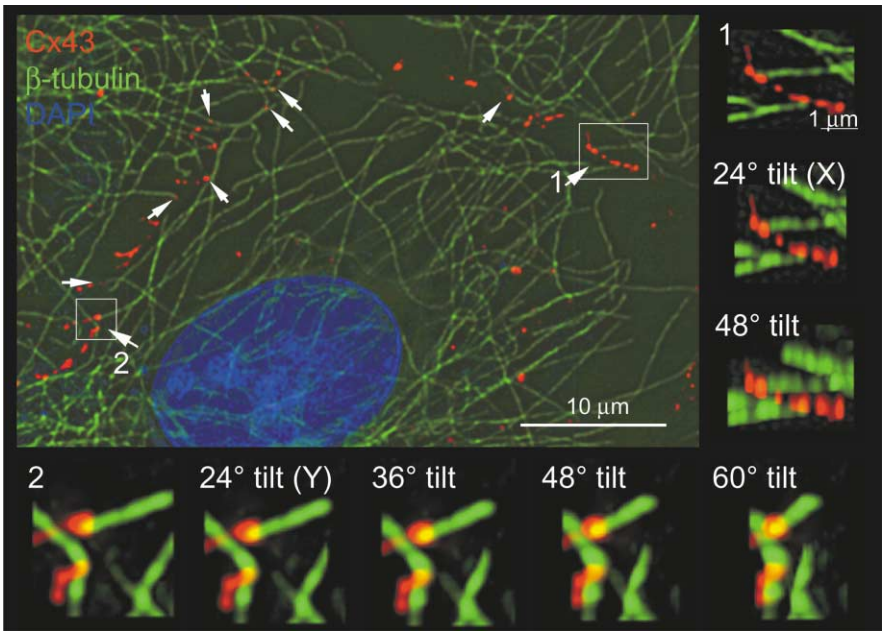

Cx43 and microtubule localization at cell-cell contacts visualized by high-resolution deconvolution microscopy. Subconfluent rat liver epithelial T51B cells were stained for Cx43 (red) and tubulin (green). It is seen that microtubules extend to and terminate at the plasma membrane only at regions of cell-cell contact (left panel; white box). High magnification of the boxed area shows that microtubules localize to Cx43 punctate structures and lower panels. Resolution enhancement by deconvolution reveals that microtubule distal ends terminate at Cx43 cell-cell contacts (right). Representative tilt projections of volume views (boxes 1 and 2) show that Cx43 and tubulin maintain their colocalization when viewed under any angle [18], consistent with microtubules interacting directly with Cx43 gap junctions (also see the Supplementary material). Note that not all Cx43 punctate structures are in contact with microtubule ends, whereas microtubules that reach the plasma membrane are in apparent contact with Cx43.

[10]. Examination of the Cx43JM sequence (Figure 3e) reveals the presence of a potential tubulin binding motif (^{234}KGVKDRVKGK^{243}; residues typically found in tubulin binding domains are underlined). This sequence is unique for Cx43 in that it is not found in other connexin family members. We addressed the specificity of microtubule binding by using the C-terminal tails of three other connexins, namely, Cx31.9, Cx46, and Cx50. No microtubule binding is detectable with those connexins (Figure 3d), consistent with tubulin binding being specific for Cx43.

To address the possible role of microtubules on Cx43-based GJC, we examined the effects of the microtubule-disrupting agent nocodazole on Rat-1 cells, which express endogenous Cx43 [4]. While microtubule disruption led to a somewhat elongated appearance of Cx43 punctate structures at cell-cell contacts (presumably due to RhoA-mediated cytoskeletal contraction [11]), functional cell-cell coupling was not significantly altered (see the Supplementary material available with this article online). Furthermore, nocodazole-treated Rat-1 cells rapidly closed their gap junctions in response to endothelin (see Supplementary material), similar to what is observed in control cells [4]. These results suggest that the microtubule cytoskeleton and, by inference, Cx43-microtubule interaction has no critical role in the regulation of Cx43 GJC. However, the possibility that microtubule disruption might lead to subtle changes in Cx43 channel gating properties cannot be excluded at present.

To visualize the Cx43-microtubule interaction in intact cells, we applied high-resolution fluorescence deconvolution microscopy. Figure 4 shows that, in contacted rat epithelial T51B cells, microtubules are organized with many distal ends extending toward the plasma membrane and terminating at Cx43-based gap junctions. Three-dimensional volume reconstructions show that endogenous Cx43 and tubulin remain colocalized under all viewing angles, consistent with a physical interaction. We note that not all Cx43 punctate structures at the plasma membrane colocalize with micotubule ends, suggesting that gap-junctional Cx43 is more abundant than peripheral microtubules. We also examined the colocalization of Cx43 and tubulin at the ultrastructural level by immunoelectron microscopy on Rat-1 cells. Gap junctions are readily distinguished by their typical morphology (Figure 5). The 15-nm gold particles, representing Cx43, are seen to decorate the entire gap-junctional plaque. Strikingly, small clusters of 10-nm gold particles, representing tubulin, are present within Cx43 gap junctions (Figure 5, arrows). Quantification in triplicate revealed that tubulin was coincident (or in very close proximity) with 47% ($\pm$ 16%) of the gap-junctional plaques analyzed (n = 39).

Our finding that microtubule distal ends terminate at Cx43 gap junctions raises the intriguing possibility that, in addition to its well-established role as a channel-forming protein, Cx43 may function as a microtubule-anchoring protein. As such, gap-junctional Cx43 might influence the properties of microtubules in contacted cells. Increasing evidence indicates that microtubule dynamics are suppressed in contacted cells, when compared to the highly dynamic behavior of microtubules in migrating cells that

Figure 5

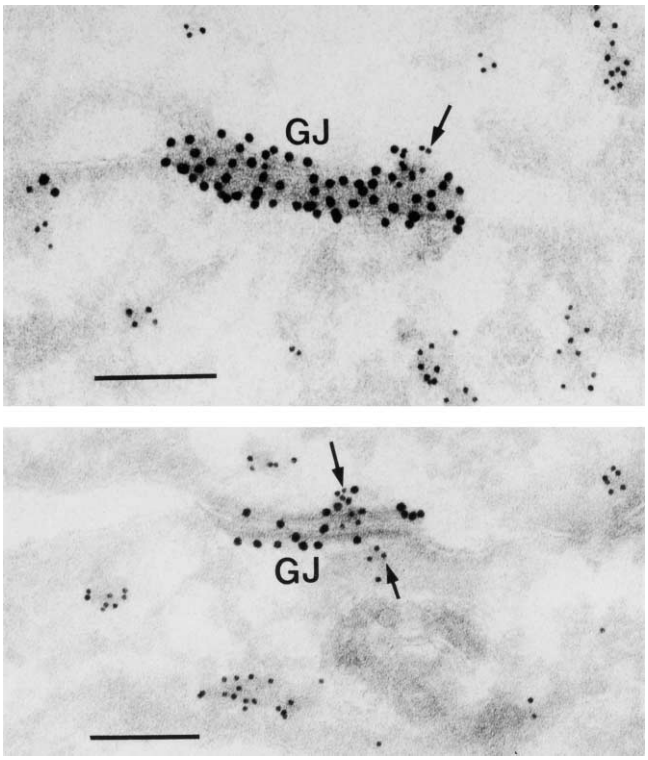

Immunoelectron microscopic localization of tubulin at Cx43 gap-junctional plaques. Electron micrographs were taken from frozen thin sections of Rat-1 fibroblasts double labeled with mouse anti-Cx43 plus 15 nm protein A-gold and rabbit anti-tubulin plus 10 nm protein A-gold (for methods, see the Supplementary material). The gap junctions (GJ) are strongly labeled for Cx43 (15 nm gold). Arrows point to tubulin staining (10 nm gold). Note that tubulin labeling is also observed in the cytoplasm; however, the fixation and sectioning procedures used for gap junction detection do not allow the visualization of microtubule bundles. The scale bar represents 200 nm.

lack cell-cell contacts [12, 13]. It has been suggested that cell-cell contact promotes the activity of an as-yet-unidentified "plus end" capping protein at the cell periphery [13] (for a review see [14]). From the present findings, it is tempting to speculate that Cx43 stabilizes microtubule plus ends at gap junctions, perhaps acting in concert with cadherins that can signal stabilization of microtubules at their minus ends near the nucleus [15]. Conceivably, altered microtubule stability could play a role in the modulation of cell motility by Cx43 and cadherins [16]. Future studies should clarify to what extent Cx43 provides a functional link between cell-cell contact formation and microtubule dynamics.

Supplementary material

Supplementary material including the Materials and methods section, additional references, and a figure showing the effects of nocodazole on gap junction morphology and cell-cell coupling is available at http://images.cellpress.com/supmat/supmatin.htm.

Acknowledgements

We thank O. Kranenburg for microtubule sedimentation assays, N. Ong for preparation of EM micrographs, and C. Waterman-Storer, J. Neefjes, and J. Vos for discussion and advice. Cx46, Cx50, and Cx31.9 GST fusion constructs were kindly provided by P. Nielsen and A. Baruch (The Scripps Research Institute). This work was supported by the Dutch Cancer Society, a UICC Fellowship (to B.G.), and National Institutes of Health grant GM55725 (to M.F.).

References

1. Goodenough DA, Goliger JA, Paul DL: **Connexins, connexons, and intercellular communication.** *Annu Rev Biochem* 1996, **65:**475-502.
2. Kumar NM, Gilula NB: **The gap junction communication channel.** *Cell* 1996, **84:**381-388.
3. Kanemitsu MY, Lau AF: **Epidermal growth factor stimulates the disruption of gap junctional communication and connexin43 phosphorylation independent of 12-0-tetradecanoylphorbol 13-acetate-sensitive protein kinase C: the possible involvement of mitogen-activated protein kinase.** *Mol Biol Cell* 1993, **4:**837-848.
4. Postma FR, Hengeveld T, Alblas J, Giepmans BN, Zondag GC, Jalink K, *et al.*: **Acute loss of cell-cell communication caused by G protein-coupled receptors: a critical role for c-Src.** *J Cell Biol* 1998, **140:**1199-1209.
5. Hossain MZ, Jagdale AB, Ao P, Kazlauskas A, Boynton AL: **Disruption of gap junctional communication by the platelet-derived growth factor is mediated via multiple signaling pathways.** *J Biol Chem* 1999, **274:**10489-10496.
6. Kanemitsu MY, Loo LW, Simon S, Lau AF, Eckhart W: **Tyrosine phosphorylation of connexin 43 by v-Src is mediated by SH2 and SH3 domain interactions.** *J Biol Chem* 1997, **272:**22824-22831.
7. Giepmans BN, Hengeveld T, Postma FR, Moolenaar WH: **Interaction of c-Src with gap junction protein connexin-43: role in the regulation of cell-cell communication.** *J Biol Chem* 2001, **276:**8544-8549.
8. Giepmans BN, Moolenaar WH: **The gap junction protein connexin-43 interacts with the second PDZ domain of the zona occludens-1 protein.** *Curr Biol* 1998, **8:**931-934.
9. Toyofuku T, Zhang H, Akamatsu Y, Kuzuya T, Tada M, Hori M: **c-Src regulates the interaction between connexin-43 and ZO-1 in cardiac myocytes.** *J Biol Chem* 2001, **276:**1780-1788.
10. Rebhan M, Brandt R, Eidenmueller J: **The microtubule interaction site.** (http://www.nbio.uni-heidelberg.de/Groups/WWW_Brandt/MT.html) 1998.
11. Ren XD, Kiosses WB, Schwartz MA: **Regulation of the small GTP-binding protein Rho by cell adhesion and the cytoskeleton.** *EMBO J* 1999, **18:**578-585.
12. Pepperkok R, Bre MH, Davoust J, Kreis TE: **Microtubules are stabilized in confluent epithelial cells but not in fibroblasts.** *J Cell Biol* 1990, **111:**3003-3012.
13. Waterman-Storer CM, Salmon WC, Salmon ED: **Feedback interactions between cell-cell adherens junctions and cytoskeletal dynamics in newt lung epithelial cells.** *Mol Biol Cell* 2000, **11:**2471-2483.
14. Schroer TA: **Microtubules don and doff their caps: dynamic attachments at plus and minus ends.** *Curr Opin Cell Biol* 2001, **13:**92-96.
15. Chausovsky A, Bershadsky AD, Borisy GG: **Cadherin-mediated regulation of microtubule dynamics.** *Nat Cell Biol* 2000, **2:**797-804.
16. Xu X, Li WE, Huang GY, Meyer R, Chen T, Luo Y, *et al.*: **Modulation of mouse neural crest cell motility by N-cadherin and connexin 43 gap junctions.** *J Cell Biol* 2001, **154:**217-230.
17. van Horck FP, Ahmadian MR, Haeusler LC, Moolenaar WH, Kranenburg O: **Characterization of p190RhoGEF: a RhoA-specific guanine nucleotide exchange factor that interacts with microtubules.** *J Biol Chem* 2001, **276:**4948-4956.
18. Falk MM: **Connexin-specific distribution within gap junctions revealed in living cells.** *J Cell Sci* 2000, **113:**4109-4120.

Supplementary material

Gap junction protein connexin-43 interacts directly with microtubules

Ben N. G. Giepmans, Ingrid Verlaan, Trudi Hengeveld, Hans Janssen, Jero Calafat, Matthias M. Falk and Wouter H. Moolenaar

Current Biology 4 September 2001, **11**:1364–1368

Supplementary materials and methods

Antibodies and chemicals

The mouse anti-Cx43 monoclonal antibody was obtained from Transduction Laboratories, rabbit anti-Cx43 and FITC-conjugated goat anti-mouse were obtained from Zymed, and Texas red-conjugated goat anti-rabbit and Lysotracker were obtained from Molecular Probes. Mouse anti-myc 9E10, anti-tubulin YL1/2, and anti-GST 2F3 were applied as hybridoma supernatants. Secondary antibodies (rabbit anti-mouse and swine anti-rabbit) conjugated to horseradish peroxidase were obtained from DAKO, and polyclonal anti-α-tubulin, monoclonal anti-β-tubulin, and nocodazole (10 μg/ml final concentration; 1000× stock in DMSO) were obtained from Sigma.

cDNA constructs and GST fusion protein purification

Cx43Myc (aa 1–382), Cx43JMMyc (aa 1–263), and GST-Cx43CT have been described before [S1, S2]. Cx43ΔJMMyc (aa 1–228/263–382), GST-Cx43JM, and GST-Cx43ΔJM were constructed with conventional molecular biology tools (PCR and restriction/ligation cloning). The proteins expressed by these plasmids are schematically shown in Figure 1. GST-Cx31.9CT (aa 209–end), GST-Cx46CT (aa 221–end), and GST-Cx50CT (aa 222–end) represent GST fusions with the C-terminal tails of these connexins, starting directly after the transmembrane domain (a glutamate residue that is conserved among all connexins). The GST-DHPH protein derived from p190RhoGEF [S3] was used as a control. GST fusion proteins were isolated from DH5α bacteria induced with IPTG according to standard procedures.

Cell culture, labeling, and transfections

Rat-1 fibroblasts, T51B rat liver epithelial cells, and COS7 cells were cultured in DMEM supplemented with 8% fetal-calf serum and 100 U/ml penicillin/streptomycin. Prior to metabolic labeling, cells were starved for 4 hr in Met/Cys-free medium. Labeling was performed with 100 μCi ^{35}S-Met/Cys for 16 hr (Amersham). Prior to measuring GJC, cells were serum-starved overnight. COS7 transfection experiments were performed using the standard DEAE-dextran transfection method, using 1 μg plasmid DNA per 10^5 cells.

GST pull-down assays

Cells were lysed in ice-cold Tx100 lysis buffer (150 mM NaCl, 50 mM TrisCl [pH 7.4], 2 mM EGTA, and 0.1% Triton X-100) supplemented with protease inhibitors (leupeptin, aprotinin, and pefabloc). All subsequent steps were performed at 4°C. Lysates were clarified for 10 min in an Eppendorf centrifuge. Next, lysates were further clarified by a pull-down assay using excess GST (except for the pull down in Figure 2a) and incubated with GST fusion proteins coupled to gluthathione beads for 1 hr. Beads were pelleted and washed three times, and proteins were eluted in Laemli Sample Buffer (LSB: 50 mM Tris [pH 6.8], 2% SDS, 10% glycerol, 5% β-mercaptoethanol, 0.1% bromophenol blue) and subjected to SDS-PAGE.

Protein purification and sequencing

Rat-1 cells from 10 dishes (15 cm) were lysed in ice-cold Tx100 lysis buffer. Lysates were clarified by centrifugation for 10 min in an Eppendorf centrifuge. Further clarification was done by adding excess (250 μg) GST immobilized on glutathione beads for 1 hr. Supernatants were incubated for another hour with 50 μg GST-gluthathione beads, and the beads were pelleted again. The supernatants were further incubated with 50 μg GST-Cx43CT immobilized on gluthatione beads. The latter two pull downs were washed three times in lysis buffer, boiled in LSB, and subjected to SDS-PAGE. Proteins were stained with Coomassie brilliant blue, and the major 55-kDa band was isolated from the gel and was trypsin digested. Three internal peptides were purified by HPLC and subjected to Edman degradation (Eurosequence).

SDS-PAGE, iso-electric focusing, autoradiography, and immunoblotting

Samples in LSB were subjected to SDS-PAGE (either 12.5% gels or 7.5%–20% gradient gels) and transferred to nitrocellulose. The blots were blocked in 5% milk and subsequently probed with primary antibodies. Next, secondary antibodies conjungated to horseradish peroxidase were incubated. Blots were washed extensively, and immunostained proteins were visualized using Enhanced ChemoLuminescence (Amersham). Two-dimensional iso-electric focusing/SDS-PAGE was performed according to standard procedures.

In vitro polymerization of microtubules and high-speed fractionation

Microtubules were made in vitro according to the manufacturer's instructions (Cytoskeleton). Microtubules were incubated for 30 min at 37°C with the indicated proteins or lysates and pelleted for 1 hr at 10,000 × g. Supernatant and pellet fractions were dissolved in LSB and subjected to SDS-PAGE.

Gap-junctional communication assay

Confluent Rat-1 cells were microinjected with a pipette solution of 5 mM Lucifer yellow (LY) and 0.1 mg/ml ethidium bromide (for identification of successfully injected cells). Intercellular LY diffusion was quantified at 3 min postinjection.

Immunofluorescence microscopy

Confocal laser scanning microscopy (CLSM) was performed on a LEICA system. After nocodazole treatment, cells were washed once with ice-cold PBS and fixed in ice-cold methanol for 20 min. Blocking (30 min) was done in PBSA (PBS; 2% BSA) at room temperature. Subsequently, cells were incubated with monoclonal anti-tubulin and polyclonal Cx43 antibodies and FITC- or Texas red-coupled secondary antibodies. Chromatin was stained blue with DAPI. High-resolution fluorescence microscopic analysis was performed on a DeltaVision Model 283 deconvolution microscope system (Applied Precision). Ten images (spaced 0.2 μm) were made, covering the entire depth of the cell periphery. Images were deconvolved, and volume views were reconstructed from the image stacks using softWoRx computer software [S4].

Immunoelectron microscopy

Rat-1 cells were fixed for 24 hr in 4% paraformaldehyde in 0.1 M PHEM buffer (pH 6.9) and then processed for ultrathin cryosectioning as previously described [S5]. Cryosections (45 nm) were cut at −125°C using diamond knives (Drukker Cuijk) in an ultracryomicrotome (Leica Aktiengesellschaft) and transferred with a mixture of sucrose and methylcellulose onto formvar-coated copper grids [S6]. The grids were placed on 35-mm petri dishes containing 2% gelatin. For double immunolabeling, the procedure described in [S7] was applied using 10- and 15-nm protein A-conjugated colloidal gold probes (EM Lab., Utrecht University). The antibodies used were rabbit anti-Cx43 and mouse anti-tubulin monoclonal antibodies (Sigma). After immunolabeling, the cryosections were embedded in a mixture of methylcellulose and uranyl acetate and examined with a Philips CM 10 electron microscope. For the controls, the primary antibody was replaced by a nonrelevant rabbit antiserum.

Figure S1

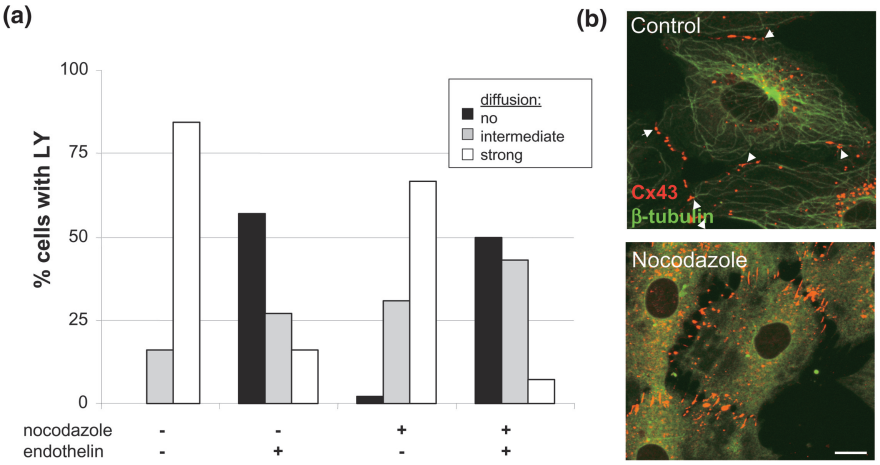

(a) Lack of effects of nocodazole on Cx43-based gap-junctional communication. Confluent Rat-1 fibroblasts were injected with Lucifer yellow (LY), and dye diffusion was measured 3 min after injection. For each data point, at least 28 cells were microinjected, and the number of cells containing LY was counted. When more than 10 cells showed LY fluorescence, GJC was considered to be maximal ("strong"; open bars). When only 1–2 cells showed LY, gap junctions were considered to be closed (black bars). When 3–10 cells showed LY after a 3-min incubation period, GJC was scored as intermediate (gray bars). In nontreated cells, LY diffuses rapidly into adjacent cells. Endothelin is a potent inhibitor of GJC. Treatment of the cells for 4 hr with nocodazole (10 μg/ml) does not affect GJC in control cells, nor does it affect endothelin-induced gap junction closure. **(b)** Effects of nocodazole on Cx43 gap junction morphology. Left panel: control Rat-1 cells display a typical radial microtubule pattern originating from the microtubule-organizing center (shown in green). Punctate Cx43-staining characteristic of gap-junctional plaques is observed at cell-cell contacts (upper panel: shown in red). In addition, vesicular Cx43 is observed in close proximity to microtubules, probably representing Cx43 transport from the endoplasmic reticulum toward the plasma membrane. Note that not all Cx43 punctate structures are in contact with microtubule ends, whereas all microtubules that reach the plasma membrane are in apparent contact with Cx43. Lower panel: Nocodazole disrupts microtubules, but does not diminish Cx43 staining at cell-cell contacts. The characteristic punctate staining of gap junctions is altered ("stretched"), probably due to nocodazole-induced contractility and stress fiber formation. The scale bar represents 10 μm.

Supplementary references

S1. Ren XD, Kiosses WB, Schwartz MA: **Regulation of the small GTP-binding protein Rho by cell adhesion and the cytoskeleton.** *EMBO J* 1999, **18:**578-585.

S2. Pepperkok R, Bre MH, Davoust J, Kreis TE: **Microtubules are stabilized in confluent epithelial cells but not in fibroblasts.** *J Cell Biol* 1990, **111:**3003-3012.

S3. van Horck FP, Ahmadian MR, Haeusler LC, Moolenaar WH, Kranenburg O: **Characterization of p190RhoGEF: a RhoA-specific guanine nucleotide exchange factor that interacts with microtubules.** *J Biol Chem* 2001, **276:**4948-4956.

S4. Falk MM: **Connexin-specific distribution within gap junctions revealed in living cells.** *J Cell Sci* 2000, **113:**4109-4120.

S5. Calafat J, Janssen H, Stahle-Backdahl M, Zuurbier AE, Knol EF, Egesten A: **Human monocytes and neutrophils store transforming growth factor-alpha in a subpopulation of cytoplasmic granules.** *Blood* 1997, **90:**1255-1266.

S6. Liou W, Geuze HJ, Slot JW: **Improving structural integrity of cryosections for immunogold labeling.** *Histochem Cell Biol* 1996, **106:**41-58.

S7. Slot JW, Geuze HJ, Gigengack S, Lienhard GE, James DE: **Immuno-localization of the insulin regulatable glucose transporter in brown adipose tissue of the rat.** *J Cell Biol* 1991, **113:**123-135.